JACS
JOURNAL OF THE AMERICAN CHEMICAL SOCIETY
Article
pubs.acs.org/JACS

Equilibrium Isotope Effects on Noncovalent Interactions in a Supramolecular Host–Guest System

Jeffrey S. Mugridge,[†,‡] Robert G. Bergman,*[,†,‡] and Kenneth N. Raymond*[,†,‡]

[†]Department of Chemistry, University of California, Berkeley, Berkeley, California 94720-1460, United States
[‡]Chemical Science Division, Lawrence Berkeley National Laboratory, Berkeley, California 94720-1460, United States

Supporting Information

ABSTRACT: The self-assembled supramolecular complex $[Ga_4L_6]^{12-}$ (**1**; L = 1,5-bis[2,3-dihydroxybenzamido]-naphthalene) can act as a molecular host in aqueous solution and bind cationic guest molecules to its highly charged exterior surface or within its hydrophobic interior cavity. The distinct internal cavity of host **1** modifies the physical properties and reactivity of bound guest molecules and can be used to catalyze a variety of chemical transformations. Noncovalent host–guest interactions in large part control guest binding, molecular recognition and the chemical reactivity of bound guests. Herein we examine equilibrium isotope effects (EIEs) on both exterior and interior guest binding to host **1** and use these effects to probe the details of noncovalent host–guest interactions. For both interior and exterior binding of a benzylphosphonium guest in aqueous solution, protiated guests are found to bind more strongly to host **1** ($K_H/K_D > 1$) and the preferred association of protiated guests is driven by enthalpy and opposed by entropy. Deuteration of guest methyl and benzyl C–H bonds results in a larger EIE than deuteration of guest aromatic C–H bonds. The observed EIEs can be well explained by considering changes in guest vibrational force constants and zero-point energies. DFT calculations further confirm the origins of these EIEs and suggest that changes in low-frequency guest C–H/D vibrational motions (bends, wags, etc.) are primarily responsible for the observed EIEs.

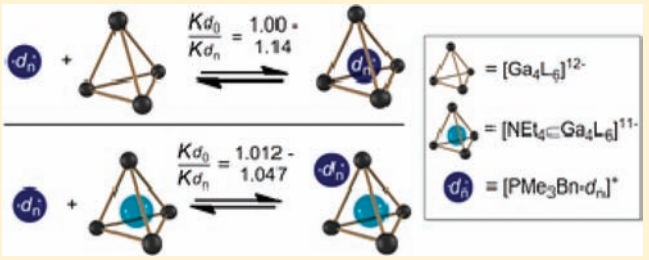

INTRODUCTION

Isotope effects (IEs) arise purely from differences in atomic mass.[1,2] Molecules differing only in their isotopic substitution, or isotopologues, have identical electronic structure, but often differ in their chemical reactivity due to changes in the vibrational frequencies and zero-point energies (ZPEs) of isotopically substituted bonds. Since isotopic substitution can perturb the thermodynamics and kinetics of chemical processes without altering the electronic energy surface of the involved molecular species, IEs provide a powerful tool to investigate the fundamental intermolecular interactions operating during chemical reactions. For this reason, numerous studies have used IEs to elucidate the mechanism of chemical reactions in both biological and chemical systems.[3]

Recently, many researchers have used IEs to probe noncovalent intermolecular interactions in supramolecular host–guest systems. These interactions, such as hydrogen bonding, CH–π, π–π, and cation–π, are often largely responsible for directing supramolecular self-assembly and host–guest recognition.[4−8] However, the weak, reversible and dynamic nature of noncovalent interactions make their relative importance and contribution to the overall free energy of molecular recognition events difficult to dissect. Isotopic substitution and the resulting kinetic and equilibrium IEs on noncovalent interactions have been successfully used to examine host–guest exchange[9,10] and binding[11−16] processes in a variety of supramolecular systems.

The self-assembled supramolecular complex $[Ga_4L_6]^{12-}$ (**1**; Figure 1; L = 1,5-bis[2,3-dihydroxybenzamido]naphthalene) can act as a host for suitably sized cationic and neutral guest molecules.[17−19] The host ligand framework generates a large, hydrophobic interior cavity (250–450 Å^3) that can encapsulate guest molecules with binding affinities of up to 10^5 M^{-1}.[20,21]

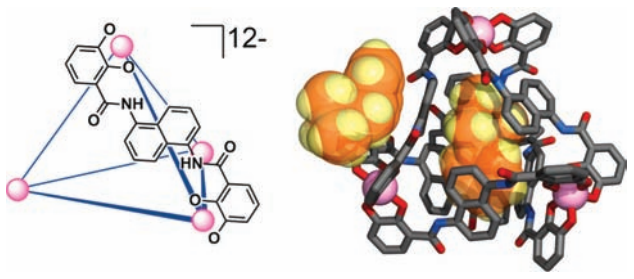

Figure 1. (Left) Schematic of host **1** with only one ligand shown for clarity. (Right) Solid-state structure of host **1** showing interior and exterior binding of NMe_3Bn^+ guest molecules (orange).

Received: July 19, 2011
Published: December 6, 2011

   dx.doi.org/10.1021/ja2067324 | J. Am. Chem.Soc. 2012, 134, 2057–2066

Cationic molecules are also bound to the negatively charged exterior of **1** with binding affinities of up to 10^2 M^{-1}.[22] We have previously used the interior space of host **1**, which differs dramatically from the bulk solvent environment, to modify the physical properties and reactivity of encapsulated guest molecules and to catalyze chemical transformations with rate accelerations of up to 10^6.[23−27] This magnitude implies that, like enzymes, the transition state of the reaction is stabilized. The specific noncovalent interactions responsible for this host−guest chemistry are difficult to study directly, however, since there are many contributions to the overall free energy of binding,[28] including both enthalpic (heats of solvation/desolvation, Coulombic attractions, and cation−π and CH−π interactions) and entropic (translational entropy, entropies of solvation/desolvation, and changes in the conformational flexibility of both host and guest upon guest binding) terms. Furthermore, small changes to guest size and shape have been shown to dramatically alter guest binding[21,29−31] and reactivity,[32−34] which precludes the use of structure−activity-type studies (*e.g.*, replacing hydrogen with fluorine atoms to alter guest electronics) to systematically investigate host−guest interactions. Thus, IEs provide a convenient and powerful method to interrogate host−guest interactions in **1** because isotopic substitution minimally changes guest structure, but gives information about how specific C−H/D bond vibrational frequencies change upon guest binding.

Recently we have examined kinetic isotope effects (KIEs) on guest exchange[35] and equilibrium isotope effects (EIEs) on exterior guest binding in supramolecular host **1**.[36] The kinetic studies revealed that deuterated $[CpRu(\eta^6\text{-}C_6H_6)]^+$-$d_n$ (Cp = η^5-cyclopentadienyl) guest molecules are displaced faster from the host cavity than their protiated isotopologues. While these KIEs are consistent with the smaller size of a C−D versus C−H bond (and might thus be called a steric isotope effect), we offered a more general explanation for the KIE based only on changes in C−H/D vibrational frequencies and ZPEs, which allows for contributions to the IE over all modes of C−H/D vibration. The observed KIEs highlight the remarkable sensitivity of the noncovalent interactions involved at the transition state to guest exchange. In a separate work, we adapted an NMR titration method originally developed by the Perrin group[37,38] for measuring IEs on acidity constants to measure very small EIEs on the exterior binding of cationic guests to host **1**. This preliminary study showed that deuterated benzylphosphonium guests bind more weakly to the exterior of **1** than their protiated isotopologues, however, this study was focused primarily on the NMR titration method and its application to our host−guest system, and the origins of the observed EIEs were not explored. Here we report a comprehensive study and analysis that well explains the thermodynamic differences in isotopologue guest binding. The EIEs on both interior and exterior binding of a number of benzylphosphonium isotopologues to host **1** were measured; protiated guest molecules are found to bind more strongly than deuterated isotopologues. These EIEs are explained by changes in guest vibrational force constants and ZPEs upon binding to host **1**. This model is further supported by DFT-level computational studies.

RESULTS AND DISCUSSION

Equilibrium Isotope Effects on Interior Guest Binding. To investigate the EIE on interior guest binding, a series of isotopologues of the guest benzyltrimethylphosphonium (**2-d_n**, Chart 1) was prepared by condensing trimethylphosphine or trimethyl-d_9-phosphine with the appropriate isotopologue of

Chart 1. Benzyltrimethyl Phosphonium Isotopologues (2-d_n)

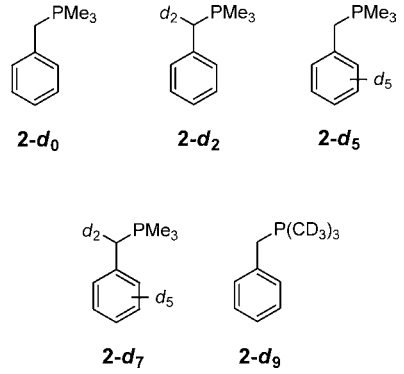

benzyl-d_n bromide. This benzylphosphonium guest was chosen for these EIE studies for several reasons: (a) it is strongly bound to the host interior (log $K_{int} \approx 4.7$ in D_2O); (b) exterior-interior equilibrium is quickly established (guest self-exchange at 300 K in D_2O is ~16 s^{-1}); (c) the guest has different functionalities (phosphonium methyl/benzyl and aromatic groups), which should each exhibit different noncovalent interactions with the host (cation−π and CH−π/π−π, respectively); and (d) a variety of isotopologues are synthetically accessible.

NMR competition titrations were carried out to measure the relative binding affinities (K_{d0}/K_{dn}) of isotopologues **2-d_n** to the interior of host **1**. Rebek and co-workers have used a similar approach to measure EIEs on guest binding in their cavitand host systems.[12] Phosphorus NMR can cleanly resolve both interior and exterior isotopologues from one another and titrations were carried out competing either **2-d_0**, **2-d_7**, and **2-d_9**, or **2-d_2**, **2-d_5**, and **2-d_9** (Figure 2); **2-d_0** could not be

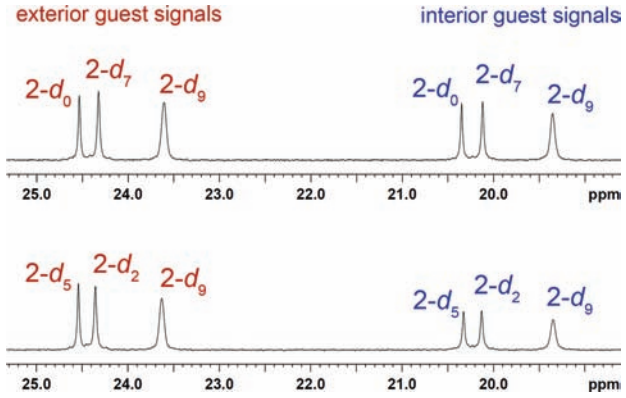

Figure 2. $^{31}P\{^1H\}$ NMR spectra from competition titrations used to determine the EIE on guest encapsulation. Spectra from NMR titrations competing **2-d_0**, **2-d_7**, and **2-d_9** (top), and **2-d_2**, **2-d_5**, and **2-d_9** (bottom) are shown. Both exterior (red) and interior (blue) **2-d_n** resonances are well resolved.

competed directly with **2-d_5** due to peak overlap in the $^{31}P\{^1H\}$ NMR spectrum. Using the relative concentrations of interior and exterior **2-d_n** isotopologues obtained from the $^{31}P\{^1H\}$ NMR spectra, linear plots were constructed to determine the EIEs on interior guest binding (Figure 3); plotting [int **2-d_0**][ext **2-d_n**] versus [int **2-d_n**][ext **2-d_0**] (where int and ext are

dx.doi.org/10.1021/ja2067324 | J. Am. Chem.Soc. 2012, 134, 2057−2066

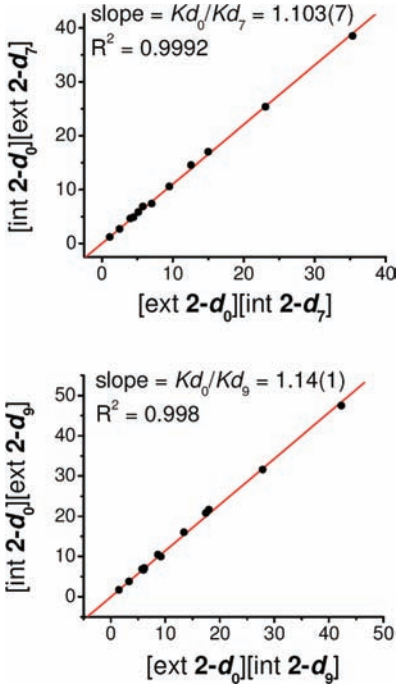

Figure 3. Linear plots used to determine EIEs (K_{d0}/K_{d7}, top; K_{d0}/K_{d9}, bottom) on interior guest binding of **2-d_n**. The plots show combined data from multiple $^{31}P\{^1H\}$ NMR titrations competing the guests **2-d_0**, **2-d_7** and **2-d_9** ([**1**] = 5−15 mM; [**2-d_n**]/[**1**] = 1.4−3.2) in D_2O at 298 K. All linear fits are fixed through zero.

interiorly and exteriorly bound species, respectively) gives a straight line with slope of the EIE (K_{d0}/K_{dn}) and intercept zero.[39]

Titrations competing guests **2-d_0**, **2-d_7**, and **2-d_9**, or **2-d_2**, **2-d_5**, and **2-d_9** were carried out over a range of guest/host ratios ([**2-d_n**]/[**1**] = 1.4−3.2) and concentrations ([**1**] = 5−15 mM), and the measured EIEs were found to be insensitive to both of these parameters, as demonstrated by the excellent linearity of the plots shown in Figure 3 (see Supporting Information for individual titration data). Table 1 lists the EIEs on interior guest binding for the isotopologues of **2-d_n**; because **2-d_0** could not be competed directly with **2-d_2** and **2-d_5**, K_{d0}/K_{d2} and K_{d0}/K_{d5} values were obtained by dividing K_{d0}/K_{d9} by K_{d2}/K_{d9} or K_{d5}/K_{d9} values, respectively. The validity of dividing EIE values and the general accuracy of the data are supported by self-consistency among independently measured EIEs: for example, taking $(K_{d0}/K_{d2})*(K_{d0}/K_{d5})$ = 1.07(2), which is very close to the measured value of 1.103(7) for K_{d0}/K_{d7}.

Table 1. EIEs on Interior Guest Binding of 2-d_n to host 1 in D_2O at 298 K

ratio	EIE	EIE/D[a]
K_{d0}/K_{d2}	1.07(1)	1.034(6)
K_{d0}/K_{d5}	1.00(2)	1.000(3)
K_{d0}/K_{d7}	1.103(7)	1.014(1)
K_{d0}/K_{d9}	1.14(1)	1.015(1)
ratio	EIE	EIE/D[a]
K_{d0}/K_{d2}	1.07(1)	1.034(6)
K_{d0}/K_{d5}	1.00(2)	1.000(3)
K_{d0}/K_{d7}	1.103(7)	1.014(1)
K_{d0}/K_{d9}	1.14(1)	1.015(1)

[a] EIE/D = $(K_{d0}/K_{dn})^{1/n}$.

All of the measured EIEs (K_{d0}/K_{dn}) on guest encapsulation for **2-d_n** are greater than or equal to 1. This means that the protiated isotopologues of benzyltrimethylphosphonium are more strongly bound to the interior of host **1** than their deuterated counterparts, with the exception of guest **2-d_5**, which showed no measurable EIE.[40] The EIE per deuterium (EIE/D) values, which are the EIEs normalized for the number of deuterium atoms in each isotopologue, show that the EIEs are larger for the methyl/benzyl C−H/D positions than for the aromatic C−H/D positions.

IEs are generally attributed to changes in bond vibrational frequencies[1,11,41−43] and the EIEs described above can be explained in terms of changes in the guests' bond vibrational frequencies, force constants and ZPEs (Figure 4). Upon encapsulation of guest **2-d_n** within **1**, attractive interactions between the guest and the aromatic walls of the host (cation−π, CH−π) lower the vibrational force constants for guest C−H/D motions. This results in lower vibrational frequencies for each of these motions and more closely spaced C−H and C−D ZPE levels when the guest is bound to the interior of **1**, than when the guest is free in aqueous solution. Smaller energy separations between the C−H and C−D ZPEs in the thermodynamically downhill encapsulated state mean that protiated guests will have a larger association constant than deuterated guests (i.e., $\Delta E_H > \Delta E_D$ in Figure 4). Thus, despite the steric consequences of encapsulation, which restrict the motional space available to bound guest molecules,[44] attractive interactions between host and guest lead to lower C−H/D vibrational force constants, or less restricted C−H/D vibrational motions, for encapsulated guest molecules.

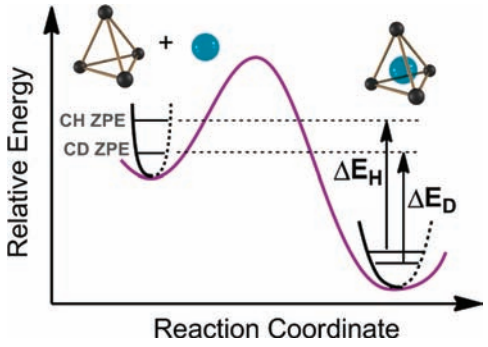

Figure 4. Diagram showing the qualitative changes in guest **2-d_n** C−H and C−D ZPEs upon binding to the interior of host **1**. Encapsulation weakens the guest vibrational force constants, illustrated above by shallower vibrational potential energy wells; this results in closer spacing of the ZPE levels for the encapsulated **2-d_n** and a larger association constant for protiated guests ($K_{d0}/K_{dn} > 1$).

Considering the EIE/D values for interior binding of **2-d_n**, the ZPE model proposed above predicts that when **2-d_n** is encapsulated in **1**, the methyl/benzyl C−H/D vibrational force constants are weakened due to attractive cation−π interactions between the positively charged phosphonium moiety and the aromatic host walls, while the vibrational force constants for the aromatic C−H/D bonds exhibit no measurable change. The larger change in vibrational frequencies for the guest's methyl/benzyl positions suggests the importance of cation−π attractive interactions between **2-d_n** and the interior of host **1**. Likewise, the lack of any EIE on guest encapsulation at the aromatic C−

dx.doi.org/10.1021/ja2067324 | J. Am. Chem.Soc. 2012, 134, 2057−2066

H/D positions suggests that CH−π and π−π interactions between the aromatic rings of **1** and **2-d_n** are a relatively small contributor to attractive host−guest interactions. However, some caution must be used here since the relative changes in vibrational frequencies and force constants depend also on the solvation environment and solvent−solute interactions between **2-d_n** and aqueous solution, and solvation of the cationic methyl/benzyl groups is undoubtedly very different than solvation of the hydrophobic aromatic group of the guest molecule. This topic is further addressed by the DFT calculations discussed near the end of this article.

The observed EIE values of $K_H/K_D > 1$ for encapsulation of guest **2-d_n** within **1** are consistent with other EIEs on noncovalent interactions that have previously been measured in aqueous solution. Aoyama et al. found EIEs of K_H/K_D = 1.08−1.12 on the binding of small, neutral molecules to the interior of their calixarene host molecules in water.[45] Thornton et al. reported IEs on the retention times of a series of nonpolar small molecules for reverse-phase HPLC experiments in methanol/water solution; they found that protiated solutes had longer retention times than deuterated solutes and interpreted these IEs as evidence of stronger attractive interactions (manifested as weaker solute vibrational frequencies) between the solute and the hydrophobic stationary phase.[43] The interior cavity of host **1** is very hydrophobic and distinct from aqueous solution, and as such, guest encapsulation might reasonably be thought of as a phase transfer, so although the RP-HPLC and supramolecular host−guest systems are very different, they do share some similarities and the IEs observed in each can be explained in fundamentally the same way.

Our results and those described above for guest binding in polar, aqueous solution stand in contrast to many examples reported for EIEs on guest encapsulation in nonpolar, organic solvent. For example, the Rebek group observed EIEs of K_H/K_D = 0.83−0.75 on the encapsulation of *p*-xylene isotopologues within their cylindrical cavitand hosts in mesitylene solution.[12] These EIEs were explained by a computer model in which an increase in C−H stretching frequencies of the xylene guest occurred upon encapsulation (the guest and host were simplified to a molecule of methane and benzene, respectively).[11] Similarly, Haino et al. reported EIEs of $K_H/K_D < 1$ for encapsulation of neutral, aliphatic and aromatic guests in a calixarene-based host in chloroform solution.[14] The authors here argued that an increase in the barrier to guest methyl group internal rotations was responsible for the observed EIEs. While it is difficult to draw very detailed conclusions from the limited number of reported EIEs on guest encapsulation in aqueous and organic solvent, it is clear that both specific, host−guest noncovalent interactions as well as guest solvation play a crucial role in determining how guest vibrational frequencies change upon encapsulation.

Equilibrium Isotope Effects on Exterior Guest Binding. Cationic guest molecules can also bind to the exterior of host **1** (Figure 1), and like interior binding, exterior association involves a variety of noncovalent host−guest interactions.[20] Exterior guest binding is generally much weaker than interior binding, with association constants of $K_{ext} = 10^2 - 10^3$ M^{-1} for monocationic guest molecules.[22] Exchange between free and exteriorly bound guest molecules is rapid on the NMR time scale. Therefore, only a single NMR resonance is observed for unencapsulated guests, which is a weighted average of the guest's chemical shift in bulk solution and its chemical shift bound to the host exterior. These characteristics of exterior guest binding make measurement of EIEs on that process challenging, since: (a) the weak binding of guest molecules to the host exterior suggests that the EIEs for exterior binding are likely very small, and (b) rapid exchange between free and exteriorly bound guest precludes the use of NMR techniques that rely on integration, as were used to measure EIEs on interior binding.

We have previously reported on an NMR titration method that overcomes these difficulties and allows for the precise and accurate measurement of very small EIEs on exterior guest binding.[36] This NMR titration methodology, originally employed by the Perrin group in order to measure very small IEs on acidity constants,[37,38] relies only on changes in the chemical shifts of directly competing isotopologues to measure the relative equilibrium constants for an equilibrium that is fast on the NMR chemical shift time scale. In our version of the experiment, isotopologues of guest **2-d_n** are simultaneously titrated into an aqueous solution of host **1** in which the interior is blocked by the strongly binding and slowly exchanging guest NEt_4^+. As **2-d_n** is added to the host solution, the cationic guest binds to the exterior of **1** and the guests' $^{31}P\{^1H\}$ NMR resonances shift upfield. The changes in these $^{31}P\{^1H\}$ NMR signals are used to extract the relative exterior binding affinities for two competing isotopologues, or the EIEs on exterior association.

Very small EIEs are observed on the binding affinity of **2-d_n** to the exterior of **1** upon deuteration of the aromatic, benzyl and/or methyl positions of the phosphonium cation (Table 2).

Table 2. EIEs on Exterior Binding of 2-d_n to Host 1 in D_2O at 296 K[a]

ratio	EIE	EIE/D[c]
K_{d0}/K_{d2}	1.012(3)	1.005(1)
K_{d0}/K_{d5}	1.021(2)	1.0038(5)
K_{d0}/K_{d7}	1.0302(4)[b]	1.00426(6)
K_{d0}/K_{d9}	1.047(2)[b]	1.0051(2)
K_{d7}/K_{d9}	1.017(3)	–

[a]EIE and EIE/D values for K_{d0}/K_{d7}, K_{d0}/K_{d9}, and K_{d7}/K_{d9} are repeated from ref 36. [b]EIEs reported as a weighted average of several titrations, see Supporting Information for individual titration data. [c]EIE/D = $(K_{d0}/K_{dn})^{1/n}$.

As with the EIEs on interior binding, isotopologues **2-d_0**, **2-d_2**, and **2-d_5** were not competed directly due to peak overlap in the $^{31}P\{^1H\}$ NMR spectra, and the values for K_{d0}/K_{d2} and K_{d0}/K_{d5} were obtained by competing **2-d_2**, **2-d_5** with **2-d_9** and then taking the appropriate ratio with the independently measured K_{d0}/K_{d9}. The validity of dividing these EIEs by one another and, in general, the high precision and accuracy of these measurements, are confirmed by the outstanding agreement between the EIEs predicted from independent NMR titrations and those measured directly. For example, $(K_{d0}/K_{d9})/(K_{d0}/K_{d7}) = K_{d7}/K_{d9} = 1.016(2)$, which perfectly matches the experimentally determined EIE of $K_{d7}/K_{d9} = 1.017(3)$; similarly, $(K_{d0}/K_{d2})(K_{d0}/K_{d5}) = K_{d0}/K_{d7} = 1.033(4)$, which again nicely agrees with the experimental value of $K_{d0}/K_{d7} = 1.0302(4)$. Therefore, although many of the EIEs differ by less than 0.01, this NMR titration method can precisely and accurately discriminate these values from one another.

Deuteration of phosphonium cation **2-d_n** results in weaker binding to the exterior of host **1** ($K_H/K_D > 1$) and the EIE/D values show that the EIEs are largest when the benzyl/methyl

dx.doi.org/10.1021/ja2067324 | J. Am. Chem.Soc. 2012, 134, 2057−2066

phosphonium CH_2/CH_3 groups are deuterated. The EIEs on exterior binding of **2-d_n** are smaller in magnitude than those observed for interior binding, but the trends observed for both are identical: protiated isotopologues of **2-d_n** are bound more strongly to both the interior and exterior of host **1** and the EIEs are larger for the phosphonium C−H/D bonds than for the aromatic C−H/D bonds. This suggests that the local noncovalent interactions operating between host and guest on the exterior and interior of **1** are fundamentally the same, despite evidence that the overall driving force for guest association in each case is different (for NEt_4^+, entropy drives encapsulation and enthalpy drives exterior ion-association).[22] Although the host exterior is very hydrophilic due to its 12-charge, it also has large aromatic surfaces that give rise to noncovalent interactions such as cation−π, CH−π, and π−π, between the host and exteriorly bound guest. Therefore, it is not entirely surprising that the specific interactions between **2-d_n** and the exterior or interior of host **1** would be very similar.

Given the alikeness of interior and exterior guest binding discussed above, the EIEs on exterior binding of **2-d_n** to host **1** can be explained analogously to those observed for interior binding: upon association of **2-d_n** to the exterior of **1**, attractive interactions (cation−π, CH−π) lower the C−H/D vibrational force constants of the exteriorly bound cation, shrinking the spacing between the guest's C−H and C−D ZPE levels, resulting in more favorable association of protiated isotopologues to the host exterior (Figure 5). As with interior binding,

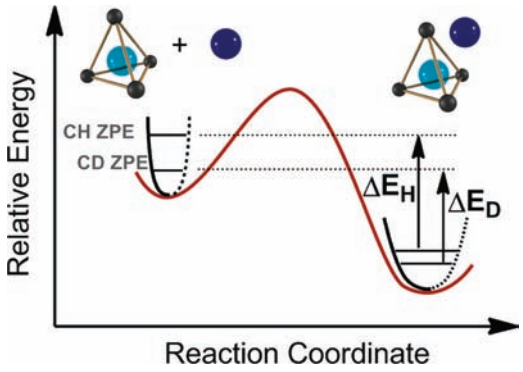

Figure 5. Diagram showing the qualitative changes in guest **2-d_n** C−H and C−D ZPEs upon binding to the exterior of host **1**. Exterior ion-association weakens the guest vibrational force constants, illustrated above by shallower vibrational potential energy wells, this results in closer spacing of the ZPE levels for the exterior bound **2-d_n** and a larger association constant for protiated guests ($K_{d0}/K_{dn} > 1$).

this resembles the IEs on RP-HPLC retention times discussed above.[43]

Temperature Dependence of the EIE on Exterior Binding. The above discussion for both interior and exterior binding of **2-d_n** to host **1** rationalizes the observed EIEs on the basis of changes in vibrational force constants and ZPE levels. However, this explanation considers only enthalpic contributions to the IE and ignores the possibility that entropy could play a role as well. The weak, reversible noncovalent interactions between host and guest are not necessarily dominated by enthalpy (as would typically be the case for primary IEs, where bonds are formed or broken) and a significant entropic contribution to the EIEs on guest binding is not unlikely.[14] To address this possibility, the thermodynamic parameters for the EIE on exterior guest binding were determined by examining the temperature dependence of the EIE. The exterior binding of **2-d_n** to **1** was chosen for this study, rather than interior binding, since the EIE values for the former are more precisely measured by NMR and experimentally easier to obtain. Since the EIEs on interior and exterior host−guest interactions follow very similar trends, as discussed above, it is likely that the thermodynamic parameters for each of these noncovalent interactions are also similar.

Aliquots of a D_2O solution of $[NEt_4 \subset \mathbf{1}]^{11-}$ were titrated into an NMR tube containing an aqueous solution of isotopologues **2-d_0**, **2-d_7**, and **2-d_9**. After each addition of host, the $^{31}P\{^1H\}$ NMR spectrum of the sample was measured at different temperatures (294−320 K) and the phosphorus chemical shifts of each isotopologue were recorded. Linearized plots were constructed from the chemical shift data to determine the EIE on exterior binding at each temperature (Table 3, see

Table 3. EIEs on Exterior Binding of 2-d_n to 1 at Different Temperatures in D_2O

T (K)	K_{d0}/K_{d7}	K_{d0}/K_{d9}
294	1.0302(4)	1.047(1)
300	1.028(1)	1.045(5)
307	1.025(1)	1.041(4)
314	1.026(1)	1.033(4)
320	1.0217(9)	1.030(4)

Supporting Information for raw NMR titration data). Van't Hoff analysis (Figure 6) revealed the thermodynamic parameters ($\Delta\Delta H$, $\Delta\Delta S$) for the EIE on exterior binding of **2-d_n** to **1** (Table 4).

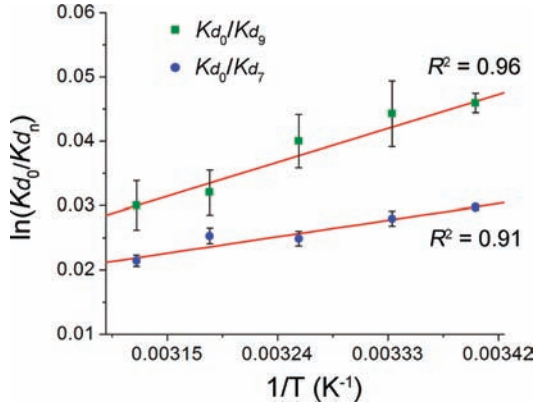

Figure 6. Van't Hoff plots for EIEs on exterior association of **2-d_0** versus **2-d_7** (blue ●) and **2-d_0** versus **2-d_9** (green ■) to host **1** in D_2O. The errors on each EIE measurement are shown; the errors on the K_{d0}/K_{d9} measurements are larger due to the much broader $^{31}P\{^1H\}$ resonance of **2-d_9**.

Table 4. Thermodynamic Parameters for the EIEs on Association of Guests 2-d_n to the Exterior of host 1 in D_2O, Obtained from a van't Hoff Analysis

ratio	$\Delta\Delta H$ (kcal/mol)	$\Delta\Delta S$ (cal/(mol K))	-T$\Delta\Delta S$ (at 298 K, kcal/mol)
K_{d0}/K_{d7}	−0.05(1)	−0.12(3)	0.04(1)
K_{d0}/K_{d9}	−0.13(2)	−0.33(5)	0.10(2)

dx.doi.org/10.1021/ja2067324 | J. Am. Chem.Soc. 2012, 134, 2057−2066

The changes in the EIEs on exterior association with temperature are small (1.030−1.022 for K_{d0}/K_{d7}; 1.047−1.030 K_{d0}/K_{d9}), but the measured EIEs are precise enough that the trends with temperature are clear and reasonable van't Hoff plots can be constructed. The $\Delta\Delta H$ and $\Delta\Delta S$ values for both K_{d0}/K_{d7} and K_{d0}/K_{d9} are negative, indicating that the preferential association of the fully protiated isotopologue, **2-d_0**, is favored by enthalpy, but opposed by entropy. Put another way, association of deuterated isotopologues to the exterior of host **1** is entropically favorable but enthalpically unfavorable. Near room temperature, the magnitudes of the opposing enthalpic ($\Delta\Delta H$) and entropic ($-T\Delta\Delta S$) terms are nearly equal, resulting in very small free energy differences ($\Delta\Delta G$ = −0.01 − −0.03 kcal/mol at 298 K) for the exterior association of **2-d_0** versus **2-d_7** or **2-d_9**.

The observation that the preferred binding of protiated isotopologues to the exterior of host **1** (*i.e.*, that $K_{d0}/K_{dn} > 1$) is driven by enthalpic changes is consistent with the vibrational force constant and ZPE model proposed above, for both exterior and interior guest association. The entropic contribution to the differential binding of isotopologues, which favors association of deuterated guests, is consistent with the changes in vibrational energy level populations expected for association of a protiated versus deuterated guest molecule. Assuming that guest association results in a decrease in guest C−H/D vibrational force constants, as proposed in the above models, a simple Boltzmann analysis reveals that there is a larger increase in the population of higher vibrational energy levels for low-frequency (wags, bends, etc.) C−D versus C−H motions in the associated guest (see Supporting Information for the details of this analysis). This equates to a greater gain in entropy for the deuterated isotopologue, consistent with the negative $\Delta\Delta S$ value observed in experiment. There are other likely contributors to the $\Delta\Delta S$ term, such as changes in the frequencies of internal bond rotations, but a detailed and quantitative deconstruction of all possible entropic contributions to the EIE is beyond the scope of the current work. Instead, we believe the qualitative analysis presented above provides a reasonable explanation for the observed thermodynamic parameters and demonstrates that the origins of these EIEs (the enthalpic and entropic contributions) can be explained by changes in vibrational force constants and ZPEs.

DFT Computational Studies. To further demonstrate that the EIEs on external or internal guest association to **1** are caused by changes in vibrational force constants and ZPEs, DFT-level calculations were carried out on model [**2-d_n**−solvent] complexes (A−D, Figure 7). Model complexes were used here since calculations at a level of theory high enough to give accurate vibrational frequencies are not feasible with the full host−guest system, due to the large number of atoms involved. Guest **2-d_0** was placed near either a molecule of naphthalene, to approximate the guest associated with the host, or a cluster of 7 water molecules,[46] to approximate the guest in free solution. The solvent groups were arbitrarily positioned either near the phosphonium methyl groups (geometries A and B, for the naphthalene and water complexes, respectively), or near the aromatic ring (geometries C and D, for the naphthalene and water complexes, respectively) of **2-d_0**. The geometries of these complexes were minimized, and the vibrational frequencies for different isotopologues of [**2-d_n**−solvent] were calculated, at the B3LYP/6-311G++(d,p) level of theory.[47] Table 5 lists the calculated ZPEs and differences in ZPEs (ΔZPE and ΔΔZPE, respectively) for isotopologues of the minimized [**2-d_n**−solvent] geometries A − D.

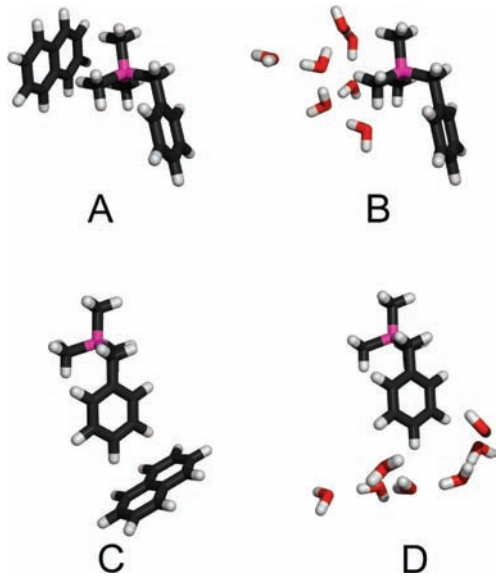

Figure 7. Optimized [**2-d_0**−solvent] geometries, B3LYP/6-311G++(d,p).

Table 5. Calculated ZPEs for Isotopologues of [2-d_n−solvent] Geometries A−D

geometry	isotopologue	ZPE (kcal/mol)	ΔZPE[a] (kcal/mol)	ΔΔZPE[b] (kcal/mol)
A	[**2-d_0**−naphthalene]	238.99	17.896	0.090
	[**2-d_9**−naphthalene]	221.09		
B	[**2-d_0**−7H_2O]	255.66	17.986	
	[**2-d_9**−7H_2O]	237.67		
C	[**2-d_0**−naphthalene]	238.76	10.306	0.034
	[**2-d_5**−naphthalene]	228.45		
D	[**2-d_0**−7H_2O]	253.75	10.339	
	[**2-d_5**−7H_2O]	243.41		

[a] ΔZPE = ZPE(**2-d_0**−X) − ZPE(**2-d_n**−X); where *X* = naphthalene or 7H_2O and *n* = 5 or 9. [b] ΔΔZPE = ΔZPE(**2-d_n**−7H_2O) − ΔZPE(**2-d_n**−naphthalene).

Comparing geometries A versus B and C versus D, in both cases the difference in ZPEs (ΔZPE) between [**2-d_0**−solvent] and [**2-d_n**−solvent] isotopologues is largest for the [**2-d_n**−7H_2O] interaction. Thinking about these ZPE changes in the context of guest exterior or interior association, the [**2-d_n**−7H_2O] geometries (B and D) represent the guest isotopologues in free solution and the [**2-d_n**−naphthalene] geometries (A and C) represent the guest isotopologues associated with host **1**. Because the [**2-d_n**−naphthalene] geometries are lower in energy than the [**2-d_n**−7H_2O] geometries (both interior and exterior guest association is thermodynamically favorable), the calculated ΔZPE values correspond to EIEs of $K_H/K_D > 1$, or more favorable association of protiated guest molecules. The predicted EIEs on moving from geometry B to A (K_{d0}/K_{d9}) or D to C (K_{d0}/K_{d5}) can be calculated from the ΔΔZPE values (EIE = exp[-ΔΔZPE/*RT*]), and these values are K_{d0}/K_{d9} = 1.16 and K_{d0}/K_{d5} = 1.06. The magnitude and direction ($K_{d0}/K_{dn} > 1$) of the computationally derived EIEs, and the larger EIE

dx.doi.org/10.1021/ja2067324 | J. Am. Chem.Soc. 2012, 134, 2057−2066

predicted for deuteration at the phosphonium methyl positions, are very much consistent with the trends in EIEs on both exterior and interior guest binding observed experimentally. This suggests that upon association of guest **2-d_n** to the exterior or interior of **1** (as approximated by interaction of the guest with naphthalene), the guest's vibrational force constants are indeed lowered from those in aqueous solution (as approximated by interaction of the guest with a cluster of water molecules), and that the resulting ZPE differences adequately explain the experimentally determined EIEs on guest binding.

These calculations also provide information about which C−H/D motions (stretching, wagging, bending, etc.) are primarily responsible for the EIEs. To determine the contributions of different vibrational modes to the EIE, the double difference of the sum of vibrational frequencies ($\Delta\Delta\Sigma\upsilon$, eq 1) for specific C−H/D motions was calculated. To clarify the meaning of $\Delta\Delta\Sigma\upsilon$, note that it is directly related to $\Delta\Delta$ZPE by eq 2, and constructing $\Delta\Delta\Sigma\upsilon$ for *all* vibrational normal modes, leads to the $\Delta\Delta$ZPE values listed in Table 5. Considering only those vibrational modes that involve motion of the methyl group H/D atoms in [**2-d_n**−solvent] geometries A and B,[48] the $\Delta\Delta\Sigma\upsilon$ values were calculated for both stretching and lower frequency vibrations. The stretching vibrations are easily separated from the other normal modes because they have much higher frequencies, but the lower frequency vibrations (bends, wags, scissors, etc.) are more difficult to separate from one another because of similar frequencies and coupling between these motions, and so are considered together. The calculated double difference vibrational sums for stretching ($\Delta\Delta\Sigma\upsilon$(stretch)) and lower frequency ($\Delta\Delta\Sigma\upsilon$(low)) $C(H/D)_3$ motions in A and B are: $\Delta\Delta\Sigma\upsilon$(stretch) = −17.15 cm^{-1} and $\Delta\Delta\Sigma\upsilon$(low) = 210.36 cm^{-1}. These values indicate that the overall EIE is opposed by changes in the phosphonium methyl group stretching vibrations, and is due instead to lower frequency vibrations such as wags, bends, rocks, etc. This is consistent with the hypothesis that changes in low frequency vibrations are at least in part responsible for the entropic component of the EIE.

$$\begin{aligned}\Delta\Delta\sum\upsilon = \{&[\sum\upsilon(\textbf{2-}\boldsymbol{d_0}{-}7H_2O)]\\ &-[\sum\upsilon(\textbf{2-}\boldsymbol{d_9}{-}7H_2O)]\}\\ &-\{[\sum\upsilon(\textbf{2-}\boldsymbol{d_0}{-}\text{naphthalene})]\\ &-[\sum\upsilon(\textbf{2-}\boldsymbol{d_9}{-}\text{naphthalene})]\}\end{aligned} \quad (1)$$

$$\Delta\Delta\text{ZPE} = \frac{1}{2}h\Delta\Delta\sum\upsilon \quad (2)$$

Carrying out a similar analysis, but now considering only those vibrational modes that involve motion of the aryl H/D atoms in [**2-d_n**−solvent] geometries C and D, the calculated double difference vibrational sums are: $\Delta\Delta\Sigma\upsilon$(stretch) = −1.66 cm^{-1} and $\Delta\Delta\Sigma\upsilon$(low) = −674.37 cm^{-1}. This suggests that both the stretching and lower frequency vibrational motions involving the aromatic C−H/D bonds in geometries C and D oppose the overall EIE. Therefore, the calculated EIEs apparently arise from changes in vibrational frequencies involving the methyl/benzyl $C(H/D)_3/C(H/D)_2$ groups, even though these bonds are not in direct contact with the solvent molecules in geometries C and D. The fact that the phosphonium methyl/benzyl groups appear to be primarily responsible for the overall EIEs, even for the **2-d_5** isotopologue, is consistent with the larger EIE values observed at those positions both experimentally (for interior and exterior guest binding) and computationally.

Conclusion. For both interior and exterior guest binding, EIEs were observed with supramolecular host **1**. For the benzyltrimethylphosphonium guest **2-d_n**, EIEs on guest interior binding range from K_{d0}/K_{dn} = 1.00−1.14 and EIEs on guest exterior binding range from K_{d0}/K_{dn} = 1.012−1.047 in aqueous solution. Protiated guests are more strongly bound than their deuterated isotopologues and the observed EIEs are largest for the phosphonium methyl/benzyl positions. The stronger binding of protiated guests is consistent with EIEs reported for similar systems in aqueous solution,[43,45] but the opposite of what has been measured for a number of different host−guest systems in organic solvent.[11,12,14] Van't Hoff analysis of the EIE on exterior binding reveals that the preferential association of protiated isotopologues is driven by enthalpy and opposed by entropy.

The EIEs on guest encapsulation and exterior association are explained by the changes in guest C−H/D vibrational force constants and ZPEs upon binding to host **1**. Association of the cationic guest to the exterior or interior of the host introduces attractive, noncovalent interactions, such as cation−π, CH−π, and π−π, which weaken guest C−H/D vibrational motions. The smaller vibrational force constants in the associated states result in closer spacing of the C−H and C−D ZPE levels, relative to aqueous solution, and this energy difference gives rise to the enthalpically favored association of protiated isotopologues. The entropic contribution to the EIE, which favors association of deuterated isotopologues, can be qualitatively explained using this same model, by considering changes in vibrational energy level populations for low frequency C−H/D motions.

DFT-level computational studies of model guest−solvent complexes mirror the trends and magnitudes of the experimentally determined EIEs. These calculations reveal that the EIEs arise from closer spacing of the ZPEs in the guest−naphthalene interaction, than in the guest-water interaction, consistent with the vibrational force constant model outlined above. Furthermore, the DFT studies indicate that the EIEs are primarily the result of changes in the low frequency vibrational motions (bends, wags, scissors, rocks, etc.) of methyl/benzyl C−H/D bonds and that the EIEs are opposed by changes in the stretching frequencies of those bonds. The importance of changes in low frequency molecular vibrations in determining the overall EIE is also consistent with the proposed explanation for the entropic contribution to the IE.

The remarkable guest stabilization, reactivity and catalysis[23−27] previously observed in supramolecular host **1** are governed in large part by noncovalent host−guest interactions. The EIEs described in this work provide a very sensitive probe with which such nonbonding associations can be dissected and explored in high detail. The measured EIEs reveal subtle differences in the interactions of different guest C−H/D bonds with the exterior and interior of host **1** and suggest the importance of attractive cation−π interactions in guest binding. These studies demonstrate that guest binding to the interior and exterior of host **1** is exquisitely sensitive to even the smallest perturbation of guest architecture and that isotopic substitution has significant effects on the noncovalent interactions that influence molecular recognition.

dx.doi.org/10.1021/ja2067324 | J. Am. Chem.Soc. 2012, 134, 2057−2066

EXPERIMENTAL SECTION

General Information. Reagents were obtained from commercial suppliers and used without further purification unless otherwise noted. All solvents were sparged with nitrogen prior to use. The K_{12}[**1**] host assembly was prepared from ligand H_4L (*N*,*N*′-(naphthalene-1,5-diyl)bis(2,3-dihydroxybenzamide)) as previously described in the literature[17] and stored under nitrogen. Compounds **2**-d_7 and **2**-d_9 were prepared as previously described.[36] All deuterated precursors were obtained from commercial suppliers with deuteration >99%.

NMR Characterization. All NMR spectra were recorded using either Bruker AV-500, AV-600 or DRX-500 spectrometers at the indicated frequencies. All ^{1}H NMR chemical shifts are reported in parts per million (δ) relative to residual protic solvent resonances. Multiplicities of ^{1}H NMR resonances are reported as *s* = singlet, *d* = doublet, *t* = triplet, *m* = multiplet and br = broad. For the NMR chemical shift data of host–guest complexes, *host* denotes signals corresponding to assembly **1** and *encaps* denotes signals corresponding to encapsulated guest; only encapsulated guest signals are tabulated. All ^{13}C{^{1}H} NMR spectra of host–guest assemblies were recorded using an HSQC experiment; 1D ^{13}C{^{1}H} NMR lacks the sensitivity necessary to obtain adequate spectra of these host–guest complexes. Only ^{13}C signals for carbon atoms attached directly to a hydrogen atom are observed in the HSQC experiment. As such, ^{13}C signals for deuterated guest carbon atoms are not reported for any host–guest complexes. All ^{31}P{^{1}H} NMR chemical shifts are referenced to an internal standard of triethylphosphate.

Mass Spectrometry Characterization. All mass spectra were recorded at the UC Berkeley Mass Spectrometry facility. Mass spectra of all host–guest assemblies were acquired on a Waters QTOF API mass spectrometer in methanol and all other mass spectra were acquired on a Thermo Scientific LTQ–Orbitrap XL mass spectrometer.

Computational Methods. All DFT calculations were carried out in the UC Berkeley Molecular Graphics and Computation Facility using Gaussian 09 software with GaussView graphical user interface.[49]

Benzyl-d_2 Trimethyl Phosphonium Bromide (2-d_2[Br]). Benzyl-d_2 bromide (0.30 mL, 1.74 mmol) was dissolved in 80 mL diethyl ether in a warm, oven-dried 250 mL of Schlenk flask. The solution was sparged with N_2 for 10 min and trimethylphosphine (0.54 mL, 5.2 mmol) was added via syringe. The solution was stirred overnight under nitrogen atmosphere and the resulting white precipitate was collected by vacuum filtration and washed with diethyl ether (3 × 30 mL). After removing residual solvent overnight under high vacuum, the product was obtained as a white solid with yield 581 mg (92%). ^{1}H NMR (600 MHz, D_2O): δ 7.47 (br, m, 3H, 3 × ArH), 7.34 (br, d, 2H, 2 × ArH), 1.83 (d, J = 14.1 Hz, 9H, PMe_3). ^{2}H NMR (92 MHz, D_2O): δ 3.7 (br, CD_2). ^{13}C{^{1}H} NMR (151 MHz, D_2O): δ 130.0 (d, J = 4.8 Hz, ArC), 129.6 (d, J = 3.0 Hz, ArC), 128.5 (d, J = 3.6 Hz, ArC), 128.3 (d, J = 8.9 Hz, ArC), 29.8 (m, CD_2), 7.1 (d, J = 55.6 Hz, PMe_3). ^{31}P{^{1}H} NMR (243 MHz, D_2O): δ 25.6 (s). MS (ESIHR) for $C_{10}H_{14}D_2P$, calcd (found) *m*/*z*: 169.1110 (169.1114).

Benzyl-d_5 Trimethyl Phosphonium Bromide (2-d_5[Br]). The title compound was prepared analogously to **2**-d_2[**Br**] from benzyl-d_5 bromide (0.35 mL, 2.97 mmol) and trimethylphosphine (0.92 mL, 8.9 mmol). The product was obtained as a white solid with yield 743 mg (99%). ^{1}H NMR (600 MHz, D_2O): δ 3.69 (d, J = 15.9 Hz, 2H, CH_2), 1.82 (d, J = 14.3 Hz, 9H, PMe_3). ^{2}H NMR (92 MHz, D_2O): δ 7.5 (br, ArD), 7.4 (br, ArD). ^{13}C{^{1}H} NMR (151 MHz, D_2O): δ 129.6 (t, J = 24 Hz, Ar**C**D), 129.0 (t, J = 25 Hz, Ar**C**D), 128.1 (d, J = 8.9 Hz, Ar**C**D), 127.9 (d, J = 25 Hz, Ar**C**), 30.1 (d, J = 50.5 Hz, **C**H_2), 6.9 (d, J = 55.3 Hz, PMe_3). ^{31}P{^{1}H} NMR (243 MHz, D_2O): δ 25.8 (s). MS (ESIHR) for $C_{10}H_{11}D_5P$, calcd (found) *m*/*z*: 172.1298 (172.1302).

General Preparation of Host–Guest Complexes K_{11}[2-d_n ⊂ 1]. All host–guest complexes with **2**-d_n were prepared *in situ*, in a nitrogen-filled glovebox, using degassed solvent. D_2O stock solutions of **2**-d_n[Br] (~50 mM) and host K_{12}[**1**] (~20 mM) were combined in the appropriate ratios (see below for titration procedure and Supporting Information for individual titration data); guest encapsulation is immediate and quantitative. Characterization details of the host–guest complexes are reported at a guest/host ratio of ~2/1.

K_{11}[2-d_0 ⊂ 1]. ^{1}H NMR (600 MHz, D_2O): δ 7.99 (d, J_{HH} = 7.8 Hz, 12H, *host* ArH), 7.68 (d, J_{HH} = 8.4 Hz, 12H, *host* ArH), 7.31 (d, J_{HH} = 7.8 Hz, 12H, *host* ArH), 6.99 (t, J_{HH} = 7.8 Hz, 12H, *host* ArH), 6.74 (d, J_{HH} = 7.2 Hz, 12H, *host* ArH), 6.59 (t, J_{HH} = 7.8 Hz, 12H, *host* ArH), 5.75 (br, 1H, *encaps* ArH), 5.05 (br, 2H, *encaps* ArH), 3.92 (br, 2H, *encaps* ArH), −0.34 (m, 2H, *encaps* CH_2), −1.26 (d, J_{PH} = 13.2 Hz, 9H, *encaps* $P(CH_3)_3$). ^{31}P{^{1}H} NMR (243 MHz, D_2O) δ 20.7 (s, *encaps* P). HRMS (ESI-QTOF): calcd (found) *m*/*z*: [**1** + **2**-d_0 + 8K$^+$]$^{3-}$ 1105.6757 (1105.6591), [**1** + **2**-d_0 + H$^+$ + 7K$^+$]$^{3-}$ 1093.0238 (1092.9905), [**1** + **2**-d_0 + 7K$^+$]$^{4-}$ 819.5160 (819.4909), [**1** + **2**-d_0 + H$^+$ + 6K$^+$]$^{4-}$ 810.0271 (810.0029), [**1** + **2**-d_0 + 2H$^+$ + 5K$^+$]$^{4-}$ 800.5381 (800.5182).

K_{11}[2-d_2 ⊂ 1]. ^{1}H NMR (600 MHz, D_2O): δ 7.96 (d, J_{HH} = 7.8 Hz, 12H, *host* ArH), 7.61 (d, J_{HH} = 8.4 Hz, 12H, *host* ArH), 7.30 (d, J_{HH} = 8.4 Hz, 12H, *host* ArH), 6.96 (m, overlapping with exterior **2**-d_2, *host* ArH), 6.73 (d, J_{HH} = 7.2 Hz, 12H, *host* ArH), 6.58 (t, J_{HH} = 7.8 Hz, 12H, *host* ArH), 5.67 (br, 1H, *encaps* ArH), 4.96 (br, 2H, *encaps* ArH), 3.87 (br, 2H, *encaps* ArH), −1.36 (d, J_{PH} = 12.6 Hz, 9H, *encaps* $P(CH_3)_3$). ^{31}P{^{1}H} NMR (243 MHz, D_2O) δ 20.2 (s, *encaps* P). HRMS (ESI-QTOF): calcd (found) *m*/*z*: [**1** + **2**-d_2 + 8K$^+$]$^{3-}$ 1106.3466 (1106.3597), [**1** + **2**-d_2 + H$^+$ + 7K$^+$]$^{3-}$ 1093.6946 (1093.6876), [**1** + **2**-d_2 + 2H$^+$ + 6K$^+$]$^{3-}$ 1080.7094 (1080.7013), [**1** + **2**-d_2 + 7K$^+$]$^{4-}$ 820.0192 (820.0231), [**1** + **2**-d_2 + H$^+$ + 6K$^+$]$^{4-}$ 810.5302 (810.5326), [**1** + **2**-d_2 + H$^+$ + 5K$^+$]$^{5-}$ 640.4316 (640.4299), [**1** + **2**-d_2 + 2H$^+$ + 4K$^+$]$^{5-}$ 632.8404 (632.8329).

K_{11}[2-d_5 ⊂ 1]. ^{1}H NMR (600 MHz, D_2O): δ 7.96 (d, J_{HH} = 7.8 Hz, 12H, *host* ArH), 7.61 (d, J_{HH} = 9.0 Hz, 12H, *host* ArH), 7.30 (d, J_{HH} = 8.4 Hz, 12H, *host* ArH), 6.95 (t, J_{HH} = 6.7 Hz, 12H, *host* ArH), 6.58 (t, J_{HH} = 7.8 Hz, 12H, *host* ArH), −0.45 (m, 2H, *encaps* CH_2), −1.36 (d, J_{PH} = 13.2 Hz, 9H, *encaps* $P(CH_3)_3$). ^{31}P{^{1}H} NMR (243 MHz, D_2O) δ 20.3 (s, *encaps* P). HRMS (ESI-QTOF): calcd (found) *m*/*z*: [**1** + **2**-d_5 + 8K$^+$]$^{3-}$ 1107.3528 (1107.3517), [**1** + **2**-d_5 + H$^+$ + 7K$^+$]$^{3-}$ 1094.7009 (1094.6860), [**1** + **2**-d_5 + H$^+$ + 6K$^+$]$^{4-}$ 811.2849 (811.2872), [**1** + **2**-d_5 + 2H$^+$ + 5K$^+$]$^{4-}$ 801.7960 (801.7955), [**1** + **2**-d_5 + H$^+$ + 5K$^+$]$^{5-}$ 641.2354 (641.2313), [**1** + **2**-d_5 + 2H$^+$ + 4K$^+$]$^{5-}$ 633.4442 (633.4349).

K_{11}[2-d_7 ⊂ 1]. ^{1}H NMR (600 MHz, D_2O): δ 7.97 (d, J_{HH} = 7.8 Hz, 12H, *host* ArH), 7.64 (d, J_{HH} = 8.4 Hz, 12H, *host* ArH), 7.30 (d, J_{HH} = 8.4 Hz, 12H, *host* ArH), 6.96 (t, J_{HH} = 8.4 Hz, 12H, *host* ArH), 6.74 (d, J_{HH} = 7.8 Hz, 12H, *host* ArH), 6.58 (t, J_{HH} = 7.8 Hz, 12H, *host* ArH), −1.33 (d, J_{PH} = 13.2 Hz, 9H, *encaps* $P(CH_3)_3$). ^{31}P{^{1}H} NMR (243 MHz, D_2O) δ 20.3 (s, *encaps* P). HRMS (ESI-QTOF): calcd (found) *m*/*z*: [**1** + **2**-d_7 + 8K$^+$]$^{3-}$ 1108.0237 (1108.0255), [**1** + **2**-d_7 + H$^+$ + 7K$^+$]$^{3-}$ 1095.3717 (1095.3804), [**1** + **2**-d_7 + 7K$^+$]$^{4-}$ 821.2770 (821.2778), [**1** + **2**-d_7 + H$^+$ + 6K$^+$]$^{4-}$ 811.5381 (811.5389), [**1** + **2**-d_7 + H$^+$ + 5K$^+$]$^{5-}$ 641.4379 (641.4271), [**1** + **2**-d_7 + 2H$^+$ + 4K$^+$]$^{5-}$ 633.8467 (633.8426).

K_{11}[2-d_9 ⊂ 1]. ^{1}H NMR (600 MHz, D_2O): δ 7.95 (d, J_{HH} = 7.8 Hz, 12H, *host* ArH), 7.61 (d, J_{HH} = 8.4 Hz, 12H, *host* ArH), 7.30 (d, J_{HH} = 7.2 Hz, 12H, *host* ArH), 6.98 (m, overlapping with exterior **2**-d_9, *encaps* ArH), 6.73 (d, J_{HH} = 7.2 Hz, 12H, *host* ArH), 6.58 (t, J_{HH} = 7.8 Hz, 12H, *host* ArH), 5.66 (br, 1H, *encaps* ArH), 4.95 (br, 2H, *encaps* ArH), 3.87 (br, 2H, *encaps* ArH), −0.46 (m, 2H, *encaps* CH_2). ^{31}P{^{1}H} NMR (243 MHz, D_2O) δ 19.4 (s, *encaps* P). HRMS (ESI-QTOF): calcd (found) *m*/*z*: [**1** + **2**-d_9 + 8K$^+$]$^{3-}$ 1108.6945 (1108.6721), [**1** + **2**-d_9 + H$^+$ + 7K$^+$]$^{3-}$ 1096.0426 (1096.0227), [**1** + **2**-d_9 + 2H$^+$ + 6K$^+$]$^{3-}$ 1083.3907 (1083.3489), [**1** + **2**-d_9 + 7K$^+$]$^{4-}$ 821.7802 (821.7579), [**1** + **2**-d_9 + H$^+$ + 6K$^+$]$^{4-}$ 812.2912 (812.2674), [**1** + **2**-d_9 + 2H$^+$ + 5K$^+$]$^{4-}$ 802.8023 (802.7799).

General Procedure for NMR Titrations to Determine EIEs on Interior Guest Binding. In a typical experiment, D_2O stock solutions of **1** (~20 mM), **2**-d_0, **2**-d_7, and **2**-d_9 (~50 mM each) were each prepared from a D_2O solution containing 1,4-dioxane (4.7 mM) and KPF_6 (100 mM) as internal standards. The stock solutions were measured by ^{1}H NMR to obtain accurate concentrations of each species and were combined in the desired ratios (see Supporting Information for individual titration conditions and data) to give a 1–2 mL solution containing **1** (~16 mM), **2**-d_0, **2**-d_7, and **2**-d_9 and the

dx.doi.org/10.1021/ja2067324 | J. Am. Chem.Soc. 2012, 134, 2057–2066

host−guest stock solution was filtered through a 0.2 μm syringe filter to remove any undissolved particulates. Different volumes (500, 400, 300, and 200 μL) of the host−guest stock solution were then added to each of four NMR tubes and diluted with D_2O (4.7 mM dioxane, 100 mM KPF_6) to a total volume of 500 μL in each tube. The set of NMR tubes (now each with different absolute concentrations, ranging from 16−6 mM) were allowed to equilibrate overnight. The concentrations of external and internal **2-d_n** isotopologues were measured by $^{31}P\{^1H\}$ NMR on a Bruker AV-600 spectrometer, relative to the KPF_6 internal standard, at 298 K using an inverse-gated decoupling sequence (zgig30) and a delay time of 7 s (the T_1 relaxation times for interior and exterior ^{31}P guest signals was ∼2.5 s; the 7 s delay should allow sufficient time for relaxation to obtain accurate integrals). Generally, ∼2 h of data collection were required to obtain adequate signal-to-noise for each $^{31}P\{^1H\}$ NMR spectrum. This procedure was repeated for different **1**:**2-d_n** ratios and the all data over a range of concentrations and host:guest ratios was combined to determine the EIEs on interior binding.

General Procedure for NMR Titrations to Determine EIEs on Exterior Guest Binding. In a typical experiment, D_2O solutions of **2-d_0** and **2-d_7** (each ∼50 mM) were combined in an NMR tube with a small amount (∼1 μL) of trimethyl phosphate as an internal standard and the volume of the tube was adjusted as necessary to ∼500 μL with D_2O. The starting concentration of **2-d_n** was generally ∼20 mM. The ratio of isotopologues (generally $[d_0]/[d_7] \approx 0.3$) was empirically chosen so that $^{31}P\{^1H\}$ peak heights remained similar to one another throughout the titration. The $^{31}P\{^1H\}$ NMR spectrum of this mixture was then measured to provide a starting chemical shift for each isotopologue. Aliquots (ranging from 5 μL − 200 μL in volume) of a D_2O solution of **1** (∼40 mM) with excess (2−5 equiv, relative to **1**) NEt_4Cl were then added to the NMR tube containing the isotopologue via syringe. After each addition the NMR tube was inverted 5−10 times to ensure adequate mixing and the $^{31}P\{^1H\}$ NMR chemical shifts of each isotopologue were measured. All chemical shifts were measured relative to that of the trimethyl phosphate internal standard. The titration is finished when addition of the **1**/NEt_4Cl solution causes no further upfield shifts in the **2-d_n** $^{31}P\{^1H\}$ resonances. All $^{31}P\{^1H\}$ NMR spectra were acquired on a Bruker AV-600 spectrometer with a delay time of 1.5 s, an acquisition time of 1.3 s and a digital resolution of 0.38 Hz/pt. For variable temperature measurements, $^{31}P\{^1H\}$ NMR spectra were collected at several different temperatures (294−320 K) after each addition of **1**; the sample was allowed to equilibrate for ∼10 min at each temperature in the NMR probe. Four scans were generally enough to obtain adequate signal-to-noise, but if more scans were needed a delay of at least 1 min was incorporated between each set of four scans to avoid any sample heating from the ^1H decoupling. Spectra were phased and calibrated (phosphate standard set to 0 ppm) manually, and the isotopologue chemical shifts were extracted by manually measuring peak centers.

■ ASSOCIATED CONTENT

Ⓢ Supporting Information

Data for NMR titrations used to determine EIE on interior guest binding, representative ^1H NMR spectrum from unsuccessful interior EIE titrations, representative $^{31}P\{^1H\}$ NMR spectra from exterior EIE titrations, data for NMR titrations used to determine EIE on exterior guest binding, error analysis used for exterior and interior EIE determination, vibrational energy level population calculation, atomic coordinates for DFT calculations, details of M06-2X DFT calculations, full citation for ref 47, and a list of references for this material. This material is available free of charge via the Internet at http://pubs.acs.org.

■ AUTHOR INFORMATION

Corresponding Author

rbergman@berkeley.edu; raymond@socrates.berkeley.edu

■ ACKNOWLEDGMENTS

The authors would like to thank Dr. Xinzheng Yang, Dr. Jamin Krinsky and Dr. Kathleen Durkin for assistance with DFT computational studies and acknowledge NSF Grants CHE-0233882 and CHE-0840505, which fund the UC Berkeley Molecular Graphics and Computational Facility. We also thank Dr. Ulla Andersen for help with mass spectrometry experiments and Prof. Charles Perrin for correspondence about his NMR titration methods. This work has been supported by the Director, Office of Science, Office of Basic Energy Sciences, and the Division of Chemical Sciences, Geosciences, and Biosciences of the U.S. Department of Energy at LBNL under Contract No. DE-AC02-05CH11231 and an NSF predoctoral fellowship to J.S.M.

■ REFERENCES

(1) Kohen, A.; Limbach, H. *Isotope Effects in Chemistry and Biology*; Taylor & Francis Group: London, 2006.
(2) Anslyn, E. V.; Dougherty, D., A. *Modern Physical Organic Chemistry*; University Science Books: Mill Valley, CA, 2006.
(3) For recent examples see: (a) Giagou, T.; Meyer, M. *Chem.—Eur. J.* **2010**, *16*, 10616−10628. (b) Zhang, H.; Wang, S.; Sun, Q.; Smith, S. C. *Phys. Chem. Chem. Phys.* **2009**, *11*, 8422−8424. (c) Stojković, V.; Kohen, A. *Isr. J. Chem.* **2009**, *49*, 163−173. (d) de La Harpe, K.; Crespo-Hernández, C. E.; Kohler, B. *J. Am. Chem. Soc.* **2009**, *131*, 17557−17559. (e) Abe, T.; Miyazawa, A.; Konno, H.; Kawanishi, Y. *Chem. Phys. Lett.* **2010**, *491*, 199−202. (f) Gonzalez-James, O. M.; Singleton, D. A. *J. Am. Chem. Soc.* **2010**, *132*, 6896−6897. (g) Liu, M.; Girma, E.; Glicksman, M. A.; Stein, R. L. *Biochemistry* **2010**, *49*, 4921−4929. (h) Wiley, K. L.; Tormos, J. R.; Quinn, D. M. *Chem. Biol. Interact.* **2010**, *187*, 124−127. For a review of IEs on noncovalent interactions, see: Wade, D. *Chem. Biol. Interact.* **1999**, *117*, 191−217.
(4) Yoshizawa, M.; Klosterman, J. K.; Fujita, M. *Angew. Chem., Int. Ed.* **2009**, *48*, 3418−3438.
(5) Saalfrank, R. W.; Maid, H.; Scheurer, A. *Angew. Chem., Int. Ed.* **2008**, *47*, 8794−8824.
(6) Oshovsky, G. V.; Reinhoudt, D. N.; Verboom, W. *ChemInform* **2007**, *38*, 2366−2393.
(7) Lehn, J.-M. *Supramolecular Chemistry: Concepts and Perspectives*; Wiley-VCH: New York, 1995.
(8) Stang, P. J.; Olenyuk, B. *Acc. Chem. Res.* **1997**, *30*, 502−518.
(9) Felder, T.; Schalley, C. A. *Angew. Chem., Int. Ed.* **2003**, *42*, 2258−2260.
(10) Liu, Y.; Warmuth, R. *Org. Lett.* **2007**, *9*, 2883−2886.
(11) Zhao, Y.-L.; Houk, K. N.; Rechavi, D.; Scarso, A.; Rebek, J. *J. Am. Chem. Soc.* **2004**, *126*, 11428−11429.
(12) Rechavi, D.; Scarso, A.; Rebek, J. *J. Am. Chem. Soc.* **2004**, *126*, 7738−7739.
(13) Tran, C. D.; Mejac, I.; Rebek, J.; Hooley, R. J. *Anal. Chem.* **2009**, *81*, 1244−1254.
(14) Haino, T.; Fukuta, K.; Iwamoto, H.; Iwata, S. *Chem.—Eur. J.* **2009**, *15*, 13286−13290.
(15) Laughrey, Z. R.; Upton, T. G.; Gibb, B. C. *Chem. Commun.* **2006**, 970−972.
(16) Liu, Y.; Warmuth, R. *Angew. Chem., Int. Ed.* **2005**, *44*, 7107−7110.
(17) Caulder, D. L.; Powers, R. E.; Parac, T. N.; Raymond, K. N. *Angew. Chem., Int. Ed.* **1998**, *37*, 1840−1843.
(18) Parac, T. N.; Caulder, D. L.; Raymond, K. N. *J. Am. Chem. Soc.* **1998**, *120*, 8003−8004.
(19) Biros, S. M.; Bergman, R. G.; Raymond, K. N. *J. Am. Chem. Soc.* **2007**, *129*, 12094−12095.
(20) Pluth, M. D.; Johnson, D. W.; Szigethy, G.; Davis, A. V.; Teat, S. J.; Oliver, A. G.; Bergman, R. G.; Raymond, K. N. *Inorg. Chem.* **2009**, *48*, 111−120.
(21) Davis, A. V.; Fiedler, D.; Seeber, G.; Zahl, A.; van Eldik, R.; Raymond, K. N. *J. Am. Chem. Soc.* **2006**, *128*, 1324−1333.

(22) Sgarlata, C.; Mugridge, J. S.; Pluth, M. D.; Tiedemann, B. E. F.; Zito, V.; Arena, G.; Raymond, K. N. *J. Am. Chem. Soc.* **2010**, *132*, 1005−1009.
(23) Wang, Z. J.; Brown, C. J.; Bergman, R. G.; Raymond, K. N.; Toste, F. D. *J. Am. Chem. Soc.* **2011**, *133*, 7358−7360.
(24) Hastings, C. J.; Pluth, M. D.; Bergman, R. G.; Raymond, K. N. *J. Am. Chem. Soc.* **2010**, *132*, 6938−6940.
(25) Brown, C. J.; Bergman, R. G.; Raymond, K. N. *J. Am. Chem. Soc.* **2009**, *131*, 17530−17531.
(26) Pluth, M. D.; Bergman, R. G.; Raymond, K. N. *Acc. Chem. Res.* **2009**, *42*, 1650−1659.
(27) Fiedler, D.; Leung, D. H.; Bergman, R. G.; Raymond, K. N. *Acc. Chem. Res.* **2005**, *38*, 349−358.
(28) Leung, D. H.; Bergman, R. G.; Raymond, K. N. *J. Am. Chem. Soc.* **2008**, *130*, 2798−2805.
(29) Hastings, C. J.; Pluth, M. D.; Biros, S. M.; Bergman, R. G.; Raymond, K. N. *Tetrahedron* **2008**, *64*, 8362−8367.
(30) Parac, T. N.; Scherer, M.; Raymond, K. N. *Angew. Chem., Int. Ed.* **2000**, *39*, 1239−1242.
(31) Pluth, M. D.; Fiedler, D.; Mugridge, J. S.; Bergman, R. G.; Raymond, K. N. *Proc. Natl. Acad. Sci. U.S.A.* **2009**, *106*, 10438−10443.
(32) Leung, D. H.; Fiedler, D.; Bergman, R. G.; Raymond, K. N. *Angew. Chem., Int. Ed.* **2004**, *43*, 963−966.
(33) Leung, D. H.; Bergman, R. G.; Raymond, K. N. *J. Am. Chem. Soc.* **2006**, *128*, 9781−9797.
(34) Pluth, M. D.; Bergman, R. G.; Raymond, K. N. *Angew. Chem., Int. Ed.* **2007**, *46*, 8587−8589.
(35) Mugridge, J. S.; Bergman, R. G.; Raymond, K. N. *Angew. Chem., Int. Ed.* **2010**, *49*, 3635−3637.
(36) Mugridge, J. S.; Bergman, R. G.; Raymond, K. N. *J. Am. Chem. Soc.* **2010**, *132*, 1182−1183.
(37) Perrin, C. L.; Fabian, M. A. *J. Am. Chem. Soc.* **1996**, *68*, 2127−2134.
(38) Perrin, C. L.; Karri, P. *J. Am. Chem. Soc.* **2010**, *132*, 12145−12149.
(39) The EIEs on interior binding of **2-d_n** to **1** were also measured using analogous ^{1}H NMR titrations. The EIEs determined this way are: K_{d0}/K_{d7} = 1.26, K_{d0}/K_{d9} = 1.03 and K_{d7}/K_{d9} = 0.97. These values are qualitatively consistent with those determined via ^{31}P NMR titrations (*i.e.* $K_{d0}/K_{dn} > 1$), but are not internally consistent: $(K_{d0}/K_{d9})/(K_{d0}/K_{d7})$ = 0.82, significantly different than the measured value of 0.97. This apparent inaccuracy in the ^{1}H NMR titration method may be due to small impurities in the ^{1}H NMR, which could not be removed (see Supporting Information, Figure S25). The ^{31}P{^{1}H} NMR resonances for the isotopologues are cleanly resolved and provide a more accurate measure of the concentrations of isotopologues on the exterior and interior of **1**. As such, only data from the ^{31}P{^{1}H} NMR titrations are considered.
(40) In a previous study on kinetic isotope effects in host **1**,[35] we measured an EIE on interior guest binding of K_{d0}/K_{d6} = 0.96(1) for the guest $[CpRu(C_6H_6)]^+$-d_n, suggesting that deuteration of the aromatic C-H bonds on the benzene ring resulted in stronger binding to the interior of host **1**. The measured value of K_{d0}/K_{d5} = 1.00(2) for interior binding of the guest **2-d_n** reported in the current study does not conclusively agree or disagree with the previous observation that deuteration of guest aromatic C−H bonds results in stronger binding to the interior of host **1**. We can only say that the EIE observed upon deuteration of the aromatic ring is small, consistent with the results reported in ref 35. Comparison of the EIEs reported here for guest **2-d_9** versus **2-d_5** also demonstrates that it is not surprising that such variation in the EIE on interior binding is observed for different guests or different guest moieties.
(41) Saunders, M.; Wolfsberg, M.; Anet, F. A. L.; Kronja, O. *J. Am. Chem. Soc.* **2007**, *129*, 10276−10281.
(42) Hayama, T.; Baldridge, K. K.; Wu, Y.-T.; Linden, A.; Siegel, J. S. *J. Am. Chem. Soc.* **2008**, *130*, 1583−1591.
(43) Turowski, M.; Yamakawa, N.; Meller, J.; Kimata, K.; Ikegami, T.; Hosoya, K.; Tanaka, N.; Thornton, E. R. *J. Am. Chem. Soc.* **2003**, *125*, 13836−13849.
(44) Mugridge, J. S.; Szigethy, G.; Bergman, R. G.; Raymond, K. N. *J. Am. Chem. Soc.* **2010**, *132*, 16256−16264.
(45) Fujimoto, T.; Yanagihara, R.; Kobayashi, K.; Aoyama, Y. *Bull. Chem. Soc. Jpn.* **1995**, *68*, 2113−2124.
(46) The choice of 7 water molecules for these calculations was based on the qualitative observation that this seemed to be the minimum but sufficient number to surround either the phosphonium or aromatic moieties and provide interactions between those groups' C-H/D bonds with nearby water molecules. Calculations with a shell of water surrounding the entire phosphonium guest were also explored, but with so many water molecules (∼50) and hence degrees of freedom the minimizations could not be made to converge. Similar calculations using only one molecule of water or one molecule benzene were also explored, and these reproduce the trends for the calculations reported in the manuscript.
(47) Geometries A and B were also minimized and vibrational frequencies calculated using M06−2X/6-311G++(d,p); the M06−2X functional has been shown to more accurately calculate energies involving significant dispersion forces: *J. Comput. Chem.***2009**, *30*, 51 . The M06−2X calculations are qualitatively consistent with the B3LYP calculations reported above, with the M06−2X functional giving an EIE of Kd_0/Kd_9 = 1.30 and $\Delta\Delta\Sigma\upsilon$(stretch) = 1.19 cm^{-1} and $\Delta\Delta\Sigma\upsilon$(low) = 1552 cm^{-1} for model systems A versus B. Like the B3LYP calculations, these closely reproduce the trends in EIEs observed experimentally and suggest that the EIEs result from changes in low frequency vibrational motions. Details of the M06−2X calculations are shown in the Supporting Information.
(48) The normal modes primarily involving vibrational motion with specific atoms were automatically selected by Gaussian09 (Gaussview) software; see ref 49.
(49) Frisch, M. J.; et al.et al. *Gaussian 09*, Revision A.02, Gaussian, Inc.: Wallingford CT, 2009.